ORIGINAL ARTICLE

Substrate binding modes and anomer selectivity of chitinase A from *Vibrio harveyi*

Wipa Suginta · Supansa Pantoom · Heino Prinz

Abstract High-performance liquid chromatography mass spectrometry (HPLC MS) was employed to assess the binding behaviors of various substrates to *Vibrio harveyi* chitinase A. Quantitative analysis revealed that hexaNAG preferred subsites −2 to +2 over subsites −3 to +2 and pentaNAG only required subsites −2 to +2, while subsites −4 to +2 were not used at all by both substrates. The results suggested that binding of the chitooligosaccharides to the enzyme essentially occurred in compulsory fashion. The symmetrical binding mode (−2 to +2) was favored presumably to allow the natural form of sugars to be utilized effectively. Crystalline α chitin was initially hydrolyzed into a diverse ensemble of chitin oligomers, providing a clear sign of random attacks that took place within chitin chains. However, the progressive degradation was shown to occur in greater extent at later time to complete hydrolysis. The effect of the reducing-end residues were also investigated by means of HPLC MS. Substitutions of Trp275 to Gly and Trp397 to Phe significantly shifted the anomer selectivity of the enzyme toward β substrates. The Trp275 mutation modulated the kinetic property of the enzyme by decreasing the catalytic constant (k_{cat}) and the substrate specificity (k_{cat}/K_m) toward all substrates by five- to tenfold. In contrast, the Trp397 mutation weakened the binding strength at subsite (+2), thereby speeding up the rate of the enzymatic cleavage toward soluble substrates but slowing down the rate of the progressive degradation toward insoluble chitin.

Abbreviations

NAG_n	β-1-4 linked oligomers of *N*-acetylglucosamine residues where $n=1$–6
DNS	Dinitrosalicylic acid
IPTG	Isopropyl thio-β-D-galactoside
PMSF	Phenylmethylsulfonylfluoride
HPLC ESI-MS	High-performance liquid chromatography electrospray mass spectrometry
ChBD	Chitin-binding domain

W. Suginta (✉) · S. Pantoom
Biochemistry–Electrochemistry Research Unit,
School of Chemistry and Biochemistry, Institute of Science,
Suranaree University of Technology,
Nakhon, Ratchasima 30000, Thailand
e-mail: wipa@sut.ac.th

H. Prinz
The Max-Planck Institute of Molecular Physiology,
Otto-Hahn-Strasse 11,
44227 Dortmund, Germany

Introduction

Chitin is a homopolymer composed of β-(1,4)-linked *N*-acetylglucosamine (GlcNAc or NAG) units and is mainly found as a structural component of fungal cell walls and exoskeletons of crustaceans and insects. A complete degradation of chitin requires chitinases (EC 3.2.1.14) and *N*-acetyl-β-glucosaminidases (EC 3.2.1.52). Chitinases are found in various organisms, and their physiological functions are dependent on the structural roles of chitin substrates existing in different species. Degradation of chitin by marine bacteria [1, 2] is crucial for maintaining the ecosystem in the marine environment [3]. In insects, chitinases are essential in the molting process and may also affect gut physiology through their involvement

in peritrophic membrane turnover [4]. Plants produce chitinases as part of their defense mechanism against distinct pathogens [5, 6], whereas fungal chitinases participate in a number of morphogenetic processes, including spore germination, side-branch formation, differentiation into spores, and autolysis [7]. Human chitinases are involved in asthma and inflammatory conditions, but the endogenous substrate(s) and the pathogenic mechanism is not yet known [8–10].

Different bacteria seem to secrete different forms of chitinases [2, 11–17]. For example, *Serratia marcescens* produces three chitinases: ChiA, ChiB, and ChiC for a synergistic degradation of chitin [18, 19], whereas *Vibrio harveyi* (formerly *Vibrio carchariae*) mainly expresses chitinase A [2]. In the CAZy database (http://www.cazy.org), *V. harveyi* chitinase A is classified as a member of family-18 glycosyl hydrolases, comprising a $(\beta/\alpha)_8$-barrel catalytic domain with a deep substrate-binding cleft and is known to catalyze the hydrolytic reaction through the 'substrate-assisted' or 'retaining mechanism' [20–26]. Most recently, the crystal structures of *V. harveyi* chitinase and its mutant E315M complexed with NAG_5 and NAG_6 were reported at 1.8–2.1 Å resolutions [27]. The structures revealed that chitooligosaccharides most likely interact with the multiple subsites of the enzyme using a linear conformation. Subsequently, the sugar chain develops a 'kink' conformation to facilitate bond cleavage. Such a movement is presumed to proceed via the 'slide and bend' mechanism [27]. The sliding motion of a chitooligomer resembles the feeding mechanism proposed by Watanabe and co-workers [28] for long-chain chitin. Either sliding or feeding, the process could be achieved only when a chitinase exhibits high processivity toward its substrates. The processivity has been described previously for other polysaccharide degrading enzymes, such as Chi A from *S. marcescens* [19, 28–30], cellobiohydrolases Cel6A from *Humicola insolens* [31], and Cel7A from *Trichoderma reesei* [32].

Insoluble substrates have been proposed to enter the active site of chitinases by the feeding mechanism and chitin oligomers by a random mechanism [28, 33]. Such a hypothesis probably holds true for most of the cases. However, a major point of concern remains the random cleavage of a chitin polymer by an endo action of chitinase A. We previously verified that *V. harveyi* chitinase A initially degraded insoluble chitins into NAG_{2-6} [20, 34]. Indeed, the production of the chitin oligomers other than NAG_2 cannot be explained as an outcome of the feeding mechanism. This is because the sliding following progressive degradation of chitin will only give rise to a single species of the product (NAG_2). In this study, we employed quantitative HPLC-MS as a direct and sensitive tool to investigate the binding behaviors of three different substrates. Together with kinetic analysis, we also demonstrated that point mutation of the reducing-end binding residues (Trp275 and Trp397) affected the substrate specificity of the tested substrates and significantly altered the anomer selectivity of *V. harveyi* chitinase A. This enzyme belongs to family-18 chitinases, which are potential drug targets for the treatment of allergic asthma.

Experimental

Bacterial strains and chemicals

The pQE 60 expression vector harboring the DNA fragment that encodes chitinase A (amino acid residues 22–597, without the 598–850 C-terminal fragment) and *Escherichia coli* type strain M15 (Qiagen, Valencia, CA, USA) were used for a high-level expression of recombinant chitinases. Chitooligosaccharides were obtained from Seikagaku Corporation (Bioactive Co., Ltd., Bangkok, Thailand). Flake chitin from crab shells was the product of Sigma-Aldrich Pte Ltd. (The Capricorn, Singapore Science Park II, Singapore). Other chemicals and reagents (analytical grade) were obtained from the following sources: reagents for bacterial media (Scharlau Chemie S.A., Barcelona, Spain.); all chemicals for protein preparation (Sigma-Aldrich Pte Ltd., Singapore and Carlo Erba Reagenti SpA, Limito, Italy); and reagents for HPLC-MS measurements (J.T. Baker, Deventer, Holland and LGC Promochem GmbH, Wesel, Germany). Milli-Q water was used for preparations of reaction buffers and for HPLC MS measurements.

Instrumentation

HPLC was operated on a 150×2.1 mm 5 μm Hypercarb®column (ThermoQuest, Thermo Electron Corporation, San Jose, CA, USA) connected to an Agilent Technologies 1100 series HPLC system (Agilent Technologies, Waldbronn, Germany) under the control of a Thermo Finnigan LTQ electrospray mass spectrometer. The proprietary program Xcalibur (Thermo Finnigan, Thermo Electron Corporation, San Jose, CA, USA) was used to control and calibrate HPLC ESI/MS. For partial hydrolysis of colloidal chitin, the electrospray MS was conducted under a positive full scan mode with a range of the mass/charge ratio (m/z) of 200–1,400. Later, the HPLC MS was run under the single ion monitoring mode for improvement of signal/noise ratios. The selected masses for detection were m/z 424.5 for NAG_2, m/z 627.5 for NAG_3, m/z 830.3 for NAG_4, m/z 1034.16 for NAG_5, and m/z 1236.3 for NAG_6. The UV signals were detected by a diode array detector between 200 and 400 nm.

Site directed mutagenesis

Point mutations were introduced to the wild-type *chitinase A* DNA that was previously cloned into the pQE60 expression vector by polymerase chain reaction (PCR) technique [20], using the QuickChange Site-Directed Mutagenesis Kit. Mutations of Trp275 to Gly and Trp397 to Phe (so as to create mutants W275G and W397F, respectively) were generated using oligonucleotides synthesized from BioServiceUnit (BSU) (Bangkok, Thailand) The forward oligonucleotide sequence used for mutagenesis of Trp275 to Gly is 5′-CATCTATCGGTGGT<u>GGA</u>A-CACTTTCTGAC-3′ and the reverse sequence is 5′-GTCA-GAAAGTGT<u>TCC</u>ACCACCGATAGATG-3′. For mutagenesis of Trp397 to Phe, the forward sequence is 5′-GACTTCTACGGCGGC<u>TTC</u>AACAACGTTCC-3′ and the reverse sequence is 5′-GGAACGTTGTT<u>GAA</u>GCCGCCG-TAGAAGTC-3′. Sequences underlined represent the mutated codons. The success of point mutations was confirmed by automated DNA sequencing (BSU, Thailand).

Recombinant expression and purification

The wild-type chitinase A with a C-terminal hexahistidine sequence was highly expressed in *E. coli* M15 cells [20]. Chitinase A mutants W275G and W397F were obtained by PCR-based site directed mutagenesis as described by Suginta et al. [35]. For recombinant expression and purification, the freshly transformed cells were grown at 37 °C in 500 mL of Luria–Bertani medium containing 100 $\mu g \cdot mL^{-1}$ ampicillin until OD_{600} reached 0.6. Then, the chitinase production was induced by the addition of 0.5 mM IPTG at 25 °C for 18 h. The cell pellet was harvested by centrifugation, re-suspended in 40 mL of lysis buffer (20 mM Tris/HCl buffer, pH 8.0, containing 150 mM NaCl, 1 mM PMSF, and 1 $mg \cdot mL^{-1}$ lysozyme), and then lysed on ice using a Sonopuls Ultrasonic homogenizer with a 6-mm-diameter probe. The supernatant obtained after centrifugation at 12,000×*g*, 45 min was applied to a Ni-NTA agarose affinity column (1.0×10 cm) (Qiagen GmbH, Hilden, Germany), washed thoroughly with 5 mM imidazole, then eluted with 250 mM imidazole in 20 mM Tris/HCl buffer, pH 8.0. An eluted fraction (10 mL) was subjected to several rounds of membrane centrifugation using Vivaspin-20 ultrafiltration membrane concentrators (M_r 10,000 cut-off, Vivascience AG, Hannover, Germany) for a complete removal of imidazole and for concentrating the proteins. Protein purity was verified on sodium dodecyl sulfate polyacrylamide gel electrophoresis as described by Laemmli [36]. A final concentration of the protein was determined by Bradford's method [37] using a standard calibration curve of bovine serum albumin (0–25 µg). The freshly prepared proteins were subjected to functional characterization or stored at −30 °C.

Partial hydrolysis of chitooligosaccharides by *V. harveyi* chitinase A

Partial hydrolysis of chitooligosaccharides by wild-type was carried out in a 50-µL reaction mixture, containing 0.1 M ammonium acetate buffer, pH 7.0, 500 µM substrate, and 100 ng purified enzyme. To minimize isomerization of the anomeric products, the reaction was performed on ice (0 °C) for 3 min, and then a 10-µL aliquot was transferred to a 200-µL sample vial and immediately subjected to HPLC MS analysis. The sample tray was kept at 4 °C, and the column was operated at 10 °C. A constant flow rate of 0.4 $mL \cdot min^{-1}$ was applied with a run time set to 15 min using a 5–70% gradient of acetonitrile, containing 0.1% formic acid. The β/α ratios were calculated from the peak areas of the corresponding products using the program Xcalibur and applying an MS Genesis algorithm for peak detection.

Time courses of chitin hydrolysis

Time-course experiments were carried out on ice in a 100-µL reaction mixture, containing 0.1 M ammonium acetate buffer, pH 7.0, 10% (*w/v*) crystalline α chitin, and 50 ng purified enzyme. Aliquots of 10 µL were taken at 0, 3, 7, 20, 30, 60, and 180 min and analyzed immediately by HPLC MS as described for chitin oligosaccharides. The peak areas, which represent total ion counts of the hydrolytic products, were quantified using the program Xcalibur applying a MS Avalon algorithm for peak detection. Standard calibration curves of NAG moieties were constructed separately from a mixture of oligosaccharide containing 0.2–500 µM of NAG_{1-6}. These data points yielded a linear curve of each standard sugar with the R^2 values of 0.9995–1.0, thus allowing molar concentrations of chitooligosacharides to be determined with confidence. For the determination of β/α contents of the chitooligosaccharide products, the reaction mixture, containing 250 ng purified enzyme in 0.1 M ammonium acetate buffer, pH 7.0, was incubated with 500 µM NAG_5 or NAG_6. Aliquots of a 100-µL reaction mixture were taken at specified times and analyzed immediately by HPLC MS. Amounts of β and α anomers of the hydrolytic products were derived from the corresponding peak areas using the standard calibration curves constructed as mentioned above.

Steady-state kinetics

Kinetic measurements were determined in a microtiter plate using NAG_5, NAG_6, and colloidal chitin as substrates. A

reaction mixture (100 μL), containing 0–500 μM substrate and chitinase (50 μg wild type, 250 μg W275G, or 0.4 μg W397F) in 0.1 M sodium acetate buffer, pH 5.5 was incubated at 37 °C for 15 min. After boiling to 100 °C for 3 min, the entire reaction mixture was subjected to the reducing sugar assay using dinitrosalicylic acid (DNS) reagent as described by Miller [38]. For colloidal chitin, the reaction was carried out the same way as the reducing-sugar assay, but concentrations of colloidal chitin was varied from 0% to 5% (w/v) and amount of enzyme was used at 150 μg wild type, 700 μg W275G, or 200 μg W397F. The amounts of the reaction products were determined from a standard curve of NAG_2 (0–500 nmol). The kinetic values were evaluated from three independent sets of data using the nonlinear regression function available in GraphPad Prism version 5.0 (GraphPad Software Inc., San Diego, CA).

Results

Structural evidence of hexaNAG in the catalytic cleft of V. harveyi chitinase A

We recently described four crystal structures of V. harveyi chitinase A and its catalytically inactive mutant E315M in complex with chitooligosaccharides (PDB codes 3BS8, 3B9A, 3B90, and 3B9E) [27]. Figure 1a is a surface representation of the catalytic domain of the mutant E315M, displaying six units of NAG (yellow) being embedded inside a long, deep-binding groove and interact specifically with various aromatic residues that stretch along the elongated cleft of the enzyme. Figure 1b represents a stick model underlying specific interactions between Tyr171 and −4NAG, Trp168 and −3 NAG, Trp275 and Trp570 and −1 to +1NAG, and Trp397 and Tyr435 with +2NAG. It is clear that the hydrophobic faces of the residues Trp275 and Trp397 stack against the heterocyclic rings of the reducing-end sugar units (+1 NAG and +2NAG; blue, Fig. 1a, b). We previously suggested that both residues are important for the primary interaction with soluble substrates [35]. We shall discuss later, in this study, that Trp275 and Trp397 are also crucial for the progressive degradation of insoluble chitin.

The structure in Fig. 1b also displays the cleavage site that is located between sites −1 and +1 (red arrow). Following the retaining mechanism, further cleavage would be expected to yield only βNAG_4 and βNAG_2. The released NAG_4 had two fates. It may diffuse into the reaction mixture and then rebind or it may slide forward to accommodate the next cleavage if remained attached to the active site. On the other hand, NAG_2 would dissociate from the product side (+1 and +2) and serves as the end product of hydrolysis.
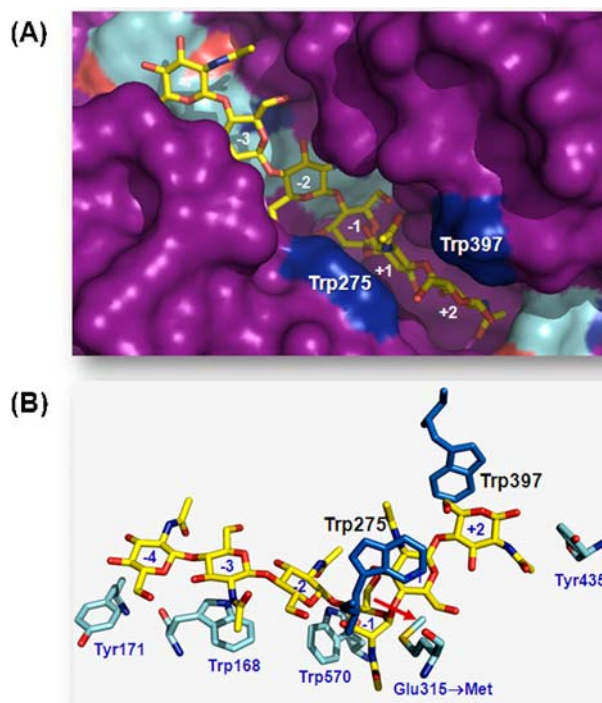

Fig. 1 The active site of V. harveyi chitinase A mutant E315M bound to hexaNAG. **a** A surface representation of hexaNAG that fully occupied subsites −4 to +2 within the substrate binding cleft of the enzyme. The sugar rings of NAG_6 are shown in *sticks*. **b** A stick model of the binding cleft of chitinase A mutant E315M complexed with NAG_6. N atoms are shown in *blue* and O atoms in *red*. C atoms are in *marine blue* for the amino acid residues and in *yellow* for the sugar residues. The cleavage site is indicated by an *arrow*, and Trp275 and Trp397 are represented in *blue*. The structure of E315M+NAG_6 complex is obtained from the PDB data base (PDB code, 3B9A) [24] and displayed by the program PyMol (http://www.pymol.org/)

Investigation of the binding modes of soluble substrates

We employed quantitative HPLC MS to establish the binding modes of three substrates. Pursuing the idea of Uchiyama et al. [28] that chitooligosaccharides randomly enter the catalytic cleft of chitinase A, it is presumed that binding of the incoming sugar chain may begin at variable sites to allow various glycosidic bonds to be accessible to the cleavage site located between sites −1 to +1. Figure 2a and b represent three possibilities where soluble substrates could interact with the multiple binding subsites of the enzyme. For a NAG_5 substrate, the binding may begin at site −4 and end at site +1, leading to a complete formation of $\beta NAG_4+\beta NAG$ (Fig. 2a, bottom trace). Alternatively, the sugar chain may bind to subsites −3 to +2, subsequently generating $\beta NAG_3+\beta NAG_2$ (Fig. 2a, middle trace) or only four units of NAG_5 bind to subsites −2 to +2, leaving the reducing-end NAG unbound at the exterior of the substrate binding cleft. As a result, βNAG_2 and either equilibrium ratio of $\beta/\alpha NAG_3$ are expected (Fig. 2a, top trace).
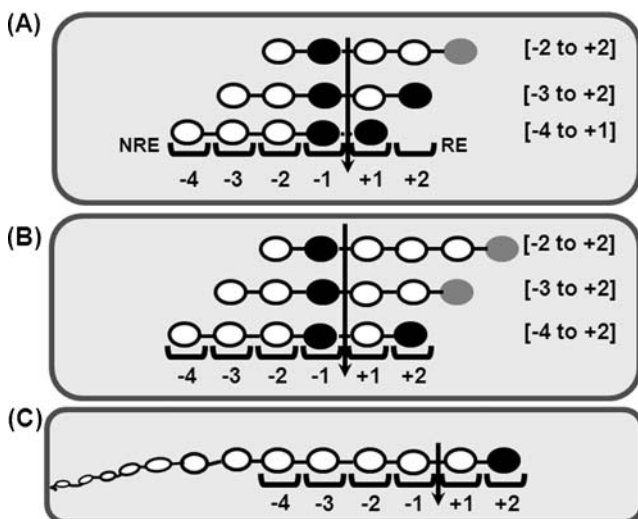
Fig. 2 Three possible models of chitin oligosaccharide bindings to the multiple binding subsites of *V. harveyi* chitinase A. Hydrolysis of **a** NAG_5, **b** NAG_6, and **c** crystalline α chitin. NAG unit with β configuration is shown in *black circle*, and NAG residue with α or β configuration with an equilibrium ratio is shown in *gray circle*. Types of the reducing-end anomers are predicted based on the retaining mechanism as suggested for family-18 chitinases

With respect to a NAG_6 substrate, it could interact with subsites (−4 to +2). This binding mode is seen in the structure of E315M+NAG_6, as shown in Fig. 1. The binding leads to a full occupancy of the six binding sites by chitohexaose (Fig. 2b, bottom trace). Subsequent bond cleavage results in the formation of βNAG_4+βNAG_2, where βNAG_2 is released from the reducing-end subsites +1 to +2. A different binding event takes place when five units of NAG_6 bind to positions (−3 to +2) (Fig. 2b, middle trace), leaving the reducing-end NAG lying empty beyond the substrate binding cleft. As a result, a single cleavage of NAG_6 leads to the formation of two NAG_3, one of which (the non-reducing end NAG_3) initially adopts β configuration, while the other NAG_3 possesses either β or α configuration. A third version of binding is that four units of NAG_6 symmetrically interact with subsites (−2 to +2), thereby letting the reducing-end NAG_2 remain unbound (Fig. 2b, top trace). This (−2 to +2) binding mode releases βNAG_2 from subsites (−2 and −1), whereas β or αNAG_4 is formed from the reducing-end side.

Assuming that the feeding mechanism is applicable, the binding characteristic of polymeric substrate is then depicted as Fig. 2c. After cleavage, a chitin chain remains attached to the active site before subsequently sliding forward toward the product side (+1 and +2), thereby allowing NAG_2 to be generated at a time. To investigate the preferred binding subsites of *V. harveyi* chitinase A, NAG_5 and NAG_6 (as a representative of soluble chitin) were partially hydrolyzed by the enzyme and the reaction mixtures analyzed immediately by HPLC MS. Partial

hydrolysis of the two substrates was carried out at 0 °C to stabilize the β and α isomers of initial products. For the assignment of the HPLC elution of α and β anomers acquired by our system, we referred to a separation profile of chitooligosaccharides obtained by reverse-phase HPLC and ^{1}H-NMR [39]. Figure 3 represents an HPLC MS separation of chitin intermediates derived from partial hydrolysis of NAG_6. The β and α forms of an individual sugar were eluted at different retention times as a doublet. The preceding peak of the doublet is identified as β and the following peak α. Further mass detection by ESI-MS assigned m/z values of the two isomers of the same sugar to be identical. For instance, m/z 424.5 was seen for $\beta\alpha NAG_2$, 627.5 for $\beta\alpha NAG_3$, 830.3 for $\beta\alpha NAG_4$, and 1,236.5 for $\beta\&\alpha NAG_6$ (Fig. 3). Peak areas representing total ion counts of the corresponding oligomers were simply converted to molar concentrations using the standard calibration curves of $NAG_{1–6}$.

From Fig. 3, *V. harveyi* chitinase A degraded NAG_6, yielding βNAG_2+βNAG_3 as major isomers. This action was observed as early as 3 min. On the other hand, βNAG_4 and αNAG_4 were detected in comparable amounts, and NAG and NAG_5 were not observed at all (Fig. 3). With NAG_5 hydrolysis, two predominant products (βNAG_2 +αNAG_3) were captured during the initial time (data not shown). No other product was seen. The preferred binding modes of the enzyme toward NAG_5 and NAG_6 were determined by comparing β content to α content of the same product (Table 1). The β contents of NAG_2, NAG_3, and NAG_4 obtained from NAG_6 hydrolysis were estimated as 90%, 65%, and 46%, respectively (Table 1, wild type). Such values do not at all fit with the β/α ratios calculated by a single binding mode as presented in Fig. 2b. Apparently, the values agree well with the values (data in
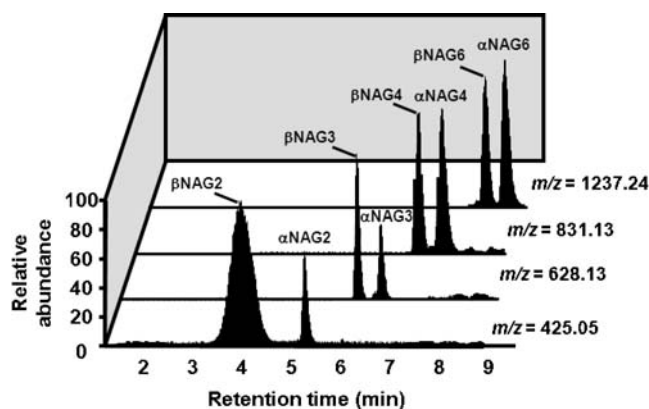

Fig. 3 An HPLC MS profile of the initial products obtained from partial hydrolysis of NAG6 by wild-type chitinase A. The hydrolytic reaction (50 μL) was carried out on ice to minimize the rate of mutarotation. After 3 min, aliquots of 10 μL of the reaction mixture were subjected to HPLC MS analysis

Table 1 Quantitative HPLC MS analysis of partial hydrolysis of chitooligosaccharides

Substrate	Enzyme	β content of initial products					
		NAG_1	NAG_2	NAG_3	NAG_4	NAG_5	NAG_6
pentaNAG (NAG5)	Wild-type	n.d.[a]	90±4.1(100)[b]	42±2.3(42)	n.d.	–	–
	W275G	n.d.	93±3.3	68±9.2	n.d.	–	–
	W397F	81±6.0	69±1.6	98±1.2	96±1.5	–	–
hexaNAG (NAG6)	Wild type	n.d.	90±2.2(100)[c]	65±3.0(71)	46±3.7(48)	–	–
	W275G	n.d.	92±4.9	63±0.7	79±2.8	–	–
	W397F	n.s.[d]	66±3.1	95±9.5	91±8.4	96±1.8	–
Crystalline α chitin	Wild type	n.d.	87±1.5(100)[e]	50±1.3(n.d.)	42±1.0(n.d)	37±0.9(n.d.)	46±4.5(n.d.)
	W275G	n.d.	88±1.2	48±2.2	56±3.2	49±5.8	50±3.7
	W397F	n.s.	88±2.1	46±1.2	57±3.4	57±1.4	51±2.0

A reaction mixture (50 µL), containing chitin substrates and chitinase A in 0.1 M ammonium acetate buffer, pH 7.0, was incubated on ice and then analyzed by HPLC ESI/MS after 3 min. The β contents were deduced from the peak areas of the corresponding products.

[a] n.d. represents product is not detectable

[b] The values in brackets are the expected values from the −2 to −2 binding mode for NAG5 hydrolysis

[c] The values in brackets are the expected values from a combination of the −3 to +2 and −2 to +2 modes for NAG6 hydrolysis

[d] n.s. represents non-separable between β and α anomer. The initial β contents were estimated from three independent sets of the experiment

[e] The value is predicted from the progressive degradation of insoluble chitin

brackets, Table 1) derived from a combination of the −2 to +2 and −3 to +2 binding modes (top and middle traces, Fig. 2b). For NAG_5 hydrolysis, the β contents of NAG_2 and NAG_3 products were predicted as 90% and 42%. These values are consistent with a single −2 to +2 binding mode (top trace, Fig. 2a). When the hydrolytic reactions were performed at equilibrium (25 °C, overnight), the predominating form of all the sugars was α. The equilibrium β contents were calculated as 48% for NAG_2, 42% for NAG_3, 41% for NAG_4, 39% for NAG_5, and 43% for NAG_6 (data not shown).

Substrate binding preference toward crystalline α chitin

The substrate binding mode of natural substrate was further investigated. Figure 4a represents a time course of the hydrolytic products generated from crystalline α chitin hydrolysis by the wild-type chitinase. Similar to previous findings [20, 34], NAG_6 was degraded by *V. harveyi* chitinase A, yielding NAG_2 major products. Other intermediates (NAG_{3-6}) were also detected in the reaction mixture as early as 3 min although in much lower concentrations. The major isomer of NAG_2 products was found to be β, while other products gave equilibrium ratios of α/β (Table 2). NAG_2 was released at least sevenfold greater than the other products over the entire range of reaction times (Fig. 4a), indicating that the enzymatic cleavage preferably took place at the second bond from the chain ends. Nevertheless, the peaks corresponding to NAG_{3-6} that were detected in the reaction mixture

simultaneously with NAG_2 verified the existence of a random attack occurring at internal points of a chitin chain.

The cleavage feature of a long-chain chitin was further elucidated. The values shown in Fig. 4b represent the cleavage ratios of NAG_2 to NAG_3–NAG_6. These values were compared when the reaction was carried out at initial time (3 min) and at equilibrium (180 min). In all cases, the cleavage ratios NAG_2 to other sugars were found to increase when the reactions reached equilibrium. For NAG_2/NAG_3, the ratio was enhanced by 1.5 times, for NAG_2/NAG_4 by nine times, for NAG_2/NAG_5 by five times, and for NAG_2/NAG_6 by six times. The lower cleavage ratios obtained at 3 min inferred that the internal attack proceeded at an early stage of reaction. The increased ratios represent the progressive action that took place at later time (i.e., at equilibrium).

Effects of point mutations on substrate bindings

Our recent data displayed a significant change in the cleavage patterns of NAG_4–NAG_6 hydrolysis when Trp275 was mutated to Gly and Trp397 to Phe. The 3D structure of chitinase A mutant E315M bound to NAG_6 has located Trp275 at the main subsites −1, and +1, and Trp397 at subsite +2 (Fig. 1a, b, blue). Alterations of the cleavage pattern as a result of Trp275 and Trp397 mutations provided a hint that both residues are important in defining the primary binding of soluble substrates [35]. In this study, we explored further how Trp275 and Trp397 influenced the binding selectivity of the enzyme. When incubated briefly,
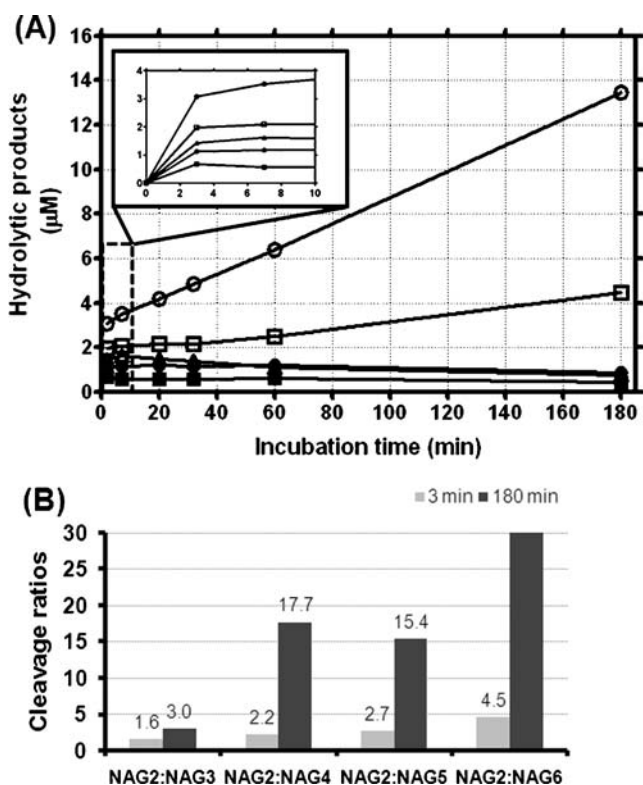
Fig. 4 Partial hydrolysis of crystalline α chitin by the wild-type chitinase A. **a** Time course of chitin hydrolysis. The hydrolytic reactions were carried out at on ice (0 °C) from 0 to 180 min and were analyzed immediately by HPLC MS. Molar concentrations of the hydrolytic products were estimated using the standard curves of NAG_{1-6}. **b** The cleavage ratios of NAG_2/NAG_{3-6} were calculated based on the molar concentration of each corresponding sugar. The reaction products generated during 0–10 min are indicated as an *inset*. *Open circle* dimers, *open square* trimers, *open triangle* tetramers; *filled circle* pentamers, *filled square* and hexamers

the mutant W275G was found to degrade NAG_5 into NAG_2 +NAG_3 with the value of βNAG_2 (93%) indistinguishable to the one formed by the wild-type enzyme (90%) (Table 1). However, the β content of NAG_3 (68%) produced by the mutated enzyme significantly increased when compared with the same product produced by the wild-type enzyme (42%). With mutant W397F, the initial products of NAG_5 hydrolysis by W397F were more varied from NAG to NAG_4. The major form of all the products produced by W397F was β with observed values of 81% for βNAG, 69% for βNAG_2, 98% for βNAG_3, and 96% βNAG_4 (Table 1).

Partial hydrolysis of NAG_6 by mutant W275G generated three product species (NAG_2+NAG_3+NAG_4), all having β major isomer. The percentages of βNAG_2 (92%) and βNAG_3 (63%) were not similar to the wild-type value (Table 1). However, βNAG_4 formed by W275G (79%) was significantly greater than βNAG_4 formed by wild type (46%). Similarly, NAG_6 hydrolysis by mutant W397F released a full range of reaction intermediates (NAG–

NAG_5). The β contents for NAG_2 (66%), NAG_3 (95%), and NAG_4 (91%) were found to be different from that obtained from the non-mutated enzyme (Table 1).

Effects of point mutations on the kinetic properties

The steady-state kinetics of the hydrolytic activity of wild-type chitinase A and mutants W275G and W397F were investigated by using the DNS reducing-sugar assay (see "Experimental"). Table 2 represents the kinetic values of the three chitinase variants against NAG_5, NAG_6, and crystalline chitin. With NAG_5 hydrolysis, the K_m of W275G (315 μM) was only slightly decreased, but the K_m of W397F (476 μM) was 1.25-fold elevated from the K_m of wild type (380 μM). Similar results were observed with NAG_6 hydrolysis, where the K_m of W275G (238 μM) was twofold lower, whereas the K_m of W397F (460 μM) was 2.6-fold greater than the K_m of wild type (174 μM).

Mutations of Trp275 and Trp397 exhibited a more severe effect on the catalytic constant (k_{cat}) of the enzyme. With the NAG_5 substrate, the k_{cat} of W275G (0.04 s^{-1}) was fivefold lower than that of wild type (0.21 s^{-1}). In contrast, the k_{cat} of W397F (2.1 s^{-1}) was tenfold higher. Similar results were seen with the NAG_6 substrate by which W275G (0.06 s^{-1}) showed a threefold decrease, but W397F displayed a 16-fold increase in the k_{cat} compared to that of wild type (0.19 s^{-1}).

Both mutations gave a different outcome on insoluble substrate. The K_m of W275G (25 mg mL^{-1}) and W397F (19 mg mL^{-1}) toward colloidal chitin were higher than that of wild type (12 mg mL^{-1}). Both mutants displayed a 0.3–0.5-fold loss in the k_{cat}. The k_{cat}/K_m values of W275G toward all substrates were decreased five times toward NAG_5 and NAG_6 but ten times toward the crystalline chitin. In contrast, the k_{cat}/K_m values of W397F toward the short-chain substrates were increased by six- to eightfold but a fivefold decrease toward the long-chain chitin.

Effects of point mutations on the anomer selectivity

The effects of Trp275 and Trp397 mutations on the anomer selectivity of the oligosaccharide hydrolysis were further investigated. Determination of substrate decrease at different time points revealed that the wild-type enzyme degraded both β and α anomers at equal rates (Fig. 5a). However, the initial rate of the depletion of βNAG_5 by W275G (Fig. 5a) occurred about 1.4 times faster than the rate of αNAG_5 depletion. At 155 min of incubation, only half of αNAG_5, but all of βNAG_5, was degraded. βNAG_5 was also utilized by mutant W397F at a significantly higher rate than αNAG_5; however, the anomer consumption varied linearly over time of incubation (Fig. 5b). At the end of reaction, a substantial amount of αNAG_5 (> 50%) and only

Table 2 Kinetic parameters of *V. harveyi* wild-type chitinase A and mutants

Chitinase A variants	pentaNAG			hexaNAG			Colloidal chitin		
	K_m (μM)	k_{cat} (s⁻¹)	k_{cat}/K_m (s⁻¹ μM⁻¹)	K_m (μM)	k_{cat} (s⁻¹)	k_{cat}/K_m (s⁻¹ μM⁻¹)	K_m (mg mL⁻¹)	k_{cat} (s⁻¹)	k_{cat}/K_m (s⁻¹ (mg mL⁻¹)⁻¹)
Wild type	380±49 (1)	0.21 (1)	5.5×10^{-4} (1)	174±23 (1)	0.19 (1)	11×10^{-4} (1)	12±1.4 (1)	0.10 (1)	83×10^{-4} (1)
W275G	315±110 (0.8)	0.04 (0.2)	1.3×10^{-4} (0.2)	238±17 (1.4)	0.06 (0.3)	2.5×10^{-4} (0.2)	25±3.7 (2.1)	0.02 (0.2)	8.0×10^{-4} (0.1)
W397F	476±11 (1.3)	2.1 (10)	44×10^{-4} (8)	460±53 (2.6)	3.0 (16)	65×10^{-4} (6)	19±0.1 (1.6)	0.03 (0.3)	16×10^{-4} (0.2)

Kinetic measurements of the hydrolytic activity of wild-type chitinase A and mutants W275G and W397F were carried out using 0–500 μM pentaNAG, hexaNAG and colloidal chitin as substrates. After 15 min of incubation at 37 °C, the amounts of the reaction products were determined by DNS assay using a standard curve constructed from NAG_2
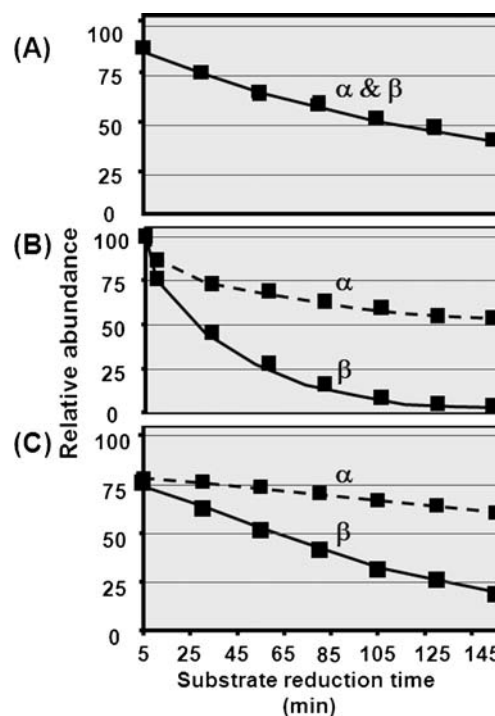
Fig. 5 Time-course of substrate consumption by chitinase A. Hydrolysis of NAG_5 by **a** wild type, **b** mutant W275G, and **c** mutant W397F. The hydrolytic reactions carried out at on ice (0 °C) from 0 to 155 min were analyzed by HPLC ESI/MS as described in texts. Rate of β anomer consumption is presented by a *black line* and rate of β anomer consumption by a *broken line*

a small amount of βNAG_5 (< 20%) remained in the reaction mixture.

With the NAG_6 substrate, similar patterns were observed (data not shown). The wild-type enzyme displayed no preferable selection toward a particular anomer of NAG_6. However, the initial rates of βNAG_6 degradation by both mutants were only slightly higher than that of αNAG_6 consumption. At the final stage of reaction, most of βNAG_5 and βNAG_6 (>80%) was used up.

Discussion

The 3D structures of the catalytically inactive mutant E315M complexed with NAG_5 and NAG_6 suggested that *V. harveyi* chitinase A most likely catalyzed chitin degradation through the 'slide and bend' mechanism [27]. From the mechanistic point of view, the sliding process can only be achieved by an enzyme with high processivity. Eijsink and colleagues reported previously that ChiA, ChiB, and ChiC from *S. marcescens* possessed different degrees of processivity [19, 29, 30]. ChiA was tested to be more processive than ChiB, whereas ChiC is a non-processive enzyme. The processive property explains how an enzyme processes it substrates. However, the mechanism

of how each substrate initially interacts with the enzyme depends entirely on the size of its substrate. Chitin oligomers are predicted to bind to the substrate-binding cleft by a random fashion. It implies that the sugar oligomer has freedom to bind to variable sites as far as the successful cleavage is concerned. In this study, three models are proposed for the productive binding of the soluble substrates (Fig. 1). NAG_5 may interact either with subsites (−4 to +1), (−3 to +2), or (−2 to +2) (Fig. 2a). Likewise, NAG_6 may bind to subsites (−4 to +2), (−3 to +2), or (−2 to +2) (Fig. 2b).

HPLC MS analysis of NAG_6 hydrolysis by wild-type chitinase gave rise to three species of reaction products ($NAG_{2,3,4}$). This happens only when the glycosidic cleavage takes place at least at two distinct locations. The presence of NAG_3 in the reaction mixture (Table 1) suggested that the enzymatic cleavage occurred in the middle of the chitin hexamer. When initial isomers of the degradation products were trapped at very low temperature (0 °C) for a short period of time (3 min), the estimated βNAG_3 (65%) agreed best to that of NAG_3 expected from the (−3 to +2) binding mode (71%) (the value in brackets, Table 1). Two other products (NAG_2 and NAG_4) could otherwise come from the interactions at subsites −4 to +2 or −2 to +2. However, the measured percentages of βNAG_2 (90%) and βNAG_4 (46%) were in conflict with the calculated values for the (−4 to +2) binding mode (100% for both βNAG_2 and βNAG_4). Instead, the obtained values agreed well with the 100% βNAG_2 and 48% βNAG_4 as calculated for the (−2 and +2) binding mode (Fig. 2b). This experimental outcome suggests binding of the chitin hexamer to either subsites −3 to +2 or −2 to +2, which emphasizes a dynamic process of interaction between an active enzyme and the substrate, and is in contrast with the occupation of the oligomer as observed in the static complex of the inactive enzyme (Fig. 1a, b). Previous quantitative HPLC MS analysis estimated the yield of NAG_3 to be 4 nmol when NAG_6 was incubated with native chitinase A for 5 min. This yield was half of NAG_2+NAG_4 yields (~8 nmol) obtained from the same reaction [34], and it indicated that NAG_6 favors the (−2 to +2) mode over the (−3 to +2) mode.

Limited hydrolysis of NAG_5 yielded only two products (NAG_2+NAG_3), meaning that the bond cleavage took place only at a single site either at positions −3 to +2 or –2 to +2 (see Fig. 2A). However, the observed percentages of βNAG_2 (90%) and βNAG_3 (42%) agreed more to that of βNAG_2 (100%) and βNAG_3 (42%) predicted for the (−2 to +2) binding mode. In contrast, 100% βNAG_2 and 100% βNAG_3 would be expected from the (−3 to +2) binding mode. No detection of NAG and NAG_4 in the reaction mixture implied that the (−4 to +1) mode was completely ignored by this substrate (see Table 1).

The binding characteristics of *S. marcescens* Chi A [40] and *Coccidioides immitis* chitinase-1 (CiX1) [41] were previously investigated by means of typical HPLC systems. Hydrolysis of NAG_6 by SmChiA that yielded 99% βNAG_2, 71% βNAG_3 and 48% βNAG_4 and hydrolysis of NAG_5 that yielded 100% βNAG_2 and 55% βNAG_3 represents the equivalent binding events as observed in this study. In CiX1, formations of $\alpha/\beta NAG_2$ (9/1) and α/βNAG4 (5/2) from NAG6 hydrolysis supports the (-2 to +2) binding mode. Sasaki et al. [42] performed a comparative study of the reaction mechanism of rice and bacterial enzymes and concluded that microbial chitinases favors the (−2)(−1)(+1)(+2)(+3)(+4) subsites, while plant chitinases prefers the (−4)(-3)(−2)(−1)(+1)(+2) subsites. Binding of a chitooligomer to (−2) to (+4) sites would be comparable to the −2 to +2 binding mode described for *V. harveyi* chitinase A.

With partial hydrolysis of insoluble chitin, NAG_2 observed as the primary product during the course of reaction (from 0 to 180 min) was mostly derived from the progressive degradation of the second bond from a chain end of chitin polymer. Imai et al. [33] demonstrated previously that the degradation of β chitin microfibrils took place from the reducing end of the sugar chain. However, other products (NAG_{3-6}) that were observed in the reaction mixture, even as early as 3 min, and the equilibrium ratios of NAG_{3-6} products obtained from a long-chain chitin hydrolysis (Table 1) were an indication of internal attacks that took place at variable positions within the chitin chain. This interpretation is further supported by the small cleavage ratios of NAG_2/NAG_{3-6} intermediates. A dramatic increase in the ratios at later time of reaction is presumably achieved quite productively with the progressive action via the feeding and sliding mechanism.

The anomer analysis revealed no selectivity of the wild-type chitinase A in utilization of α or β substrates (Fig. 5a). No selectivity of binding by all means leaves the enzyme a lot more freedom to efficiently take up the β or α substrates that are present in the reaction equilibrium. This idea is well complimented by binding of NAG_5 to subsites (−2 to +2) and NAG_6 to subsites (−3 to +2) or (−2 to +2) as seen in Fig. 2a and b. For the structural point of view, *V. harveyi* chitinase A is shown to comprise a substrate binding cleft with a long, deep groove structure (Fig. 1). The reducing end of the binding groove is shown to be open, giving adequate space for the incoming sugar chain to move beyond the +2 site. As a consequence, various glycosidic bonds are accessible to the cleavage site. The open-end active site certainly fits the binding preference of NAG_5 and NAG_6 and the endo action of the enzyme toward chitin polymers.

We previously reported that the residues Trp275 and Trp397 positioned at subsites (−1, +1, and +2 sites) are particularly essential for defining the primary binding of

soluble chitooligosaccharides and Trp70 located at the N-terminal end of the ChBD is crucial for insoluble chitin degradation [35, 43]. In this study, the effects of mutations on the kinetic properties of the enzyme were evaluated. It was found that mutations of Trp275 and Trp397 to Gly and Phe, respectively, significantly changed the substrate specificity and the anomer selectivity of the enzyme. The structure of mutant E315M bound to NAG_6 showed that Trp275 could interact strongly with −1NAG and +1NAG [27]. Mutation of this residue was found to affect the kinetic properties involving the catalytic center by decreasing the k_{cat} and the k_{cat}/K_m toward NAG_5 and NAG_6 by a magnitude of 5 (Table 2). In addition, the mutation significantly increased the apparent rate of β consumption as shown in Fig. 5a. The event may be explained as a shift of the sugar chain toward the non-reducing end in the search for other available binding sites to compensate for the loss of interactions. The observed yields of $βNAG_2$ (93%) and $βNAG_3$ (68%) obtained from the cleavage of NAG_5 by W275G (Table 1) agrees well with the predicted yields of $βNAG_2$ (100%) and $βNAG_3$ (42–100%) of the model shown in Fig. 6a. A single move of the sugar chain toward the non-reducing end is predicted as further movement would likely be blocked by high affinity of binding between the reducing end of NAG_5 and Trp397 at subsite +2.

Different situations were observed with mutant W397F. Mutation of Trp397 to Phe led to an increase in the k_{cat} toward NAG_5 and NAG_6 by 10- and16-fold, giving rise to an increase in the k_{cat}/K_m by a magnitude of 8 and 16, respectively. Trp397 is a crucial binding residue located at subsite +2, and it determines the primary binding of chitooligosaccharide substrates. A phenylalanine substitu-

tion appeared to weaken the binding strength of this subsite, enabling the sugar chain to move more freely and allowing various glycosidic bonds to be exposed to the cleavage sites. A full range of reaction intermediates seen in the reaction mixture of W397F (Table 1) supports the above assumption. Hydrolysis of NAG_5 by W397F, yielding 81% $βNAG$, 69% $βNAG_2$, 98% $βNAG_3$, and 96% $βNAG_4$ products agreed well with the yields proposed in Fig. 6b.

The residues Trp275 and Trp397 are found to be important for insoluble chitin hydrolysis, since the mutations showed a remarkable decrease in the k_{cat} value of the enzyme. The structure in Fig. 1 shows that both residues are located in a perfect position to be responsible for the feeding process by pulling the chitin chain toward the reducing end subsites, thereby permitting the next processive hydrolysis to occur (see Fig. 6c). A significant reduction of the k_{cat} and the k_{cat}/K_m values toward colloidal chitin (Table 2) seems to support the proposed roles of both residues (Table 2). Similar effects were also reported with ChiA1 from *B. circulans*, where mutations of Trp164 (equivalent to Trp275) and Trp285 (equivalent to Trp397) drastically reduced the hydrolytic activity of their enzymes toward colloidal chitin by 40–50% [44].

In conclusion, we employed quantitative HPLC MS to determine the binding modes of a family-18 chitinase from *V. harveyi* toward three substrates. Neither a random nor a progressive binding was entirely employed for a complete hydrolysis of the tested substrates. Nevertheless, soluble chitins seem to favor the −2 to +2 binding, but insoluble chitin preferred the progressive binding. Mutations of Trp275 and Trp397 were found to affect the anomer selectivity and the substrate specificity toward soluble substrates. The evaluation of the kinetic data suggested

Fig. 6 Plausible effects of point mutation on the substrate binding preference and the anomer selectivity. Binding of NAG_5 to **a** wild-type chitinase, **b** mutant W275G, and **c** mutant W397F. The β configuration is shown in *black circle*, NAG residue with α or β configuration with an equilibrium ratio is shown in *gray circle*, and NAG residue with α or β configuration that binds to a loosen-affinity binding site is shown in *gray-filled in dark circle*. The cleavage site is indicated by an *arrow*
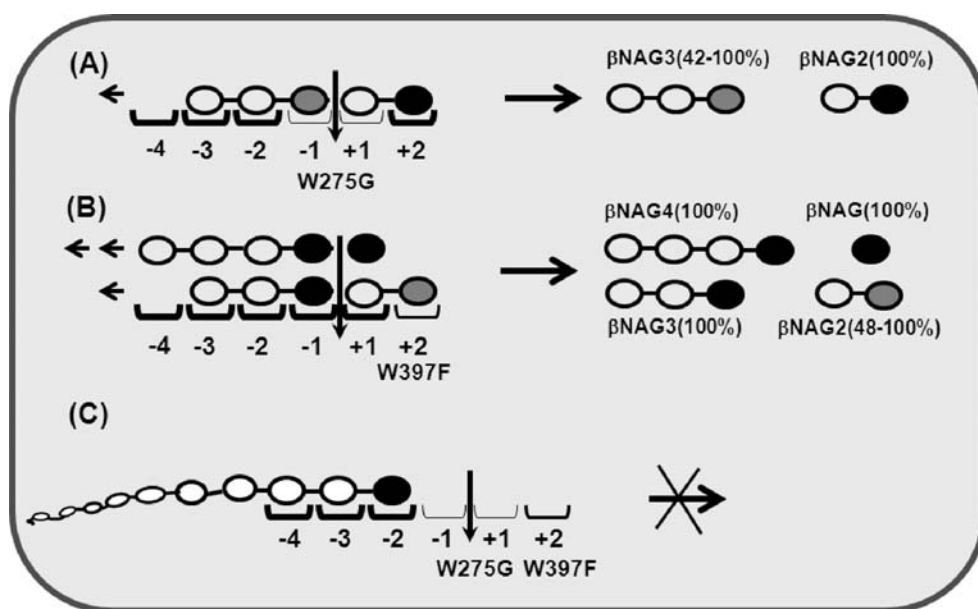
that Trp275 and Trp397 are likely involved in the feeding process that facilitates a degradation of chitin polymer in a progressive manner. Ultimately, understanding of the binding mechanism of family-18 chitinases to their substrates may aid the drug-screening program to obtain effective inhibitors that act as therapeutic candidates for successful treatment of allergic asthma.

References

1. Hirono I, Yamashita M, Aoki T (1998) Note: molecular cloning of chitinase genes from *Vibrio anguillarum* and *V. parahaemolyticus*. J Appl Microbiol 84:1175–1178
2. Suginta W, Robertson PA, Austin B et al (2000) Chitinases from *Vibrios*: activity screening and purification of chi A from *Vibrio carchariae*. J Appl Microbiol 89:76–84
3. Keyhani NO, Roseman S (1999) Physiological aspects of chitin catabolism in marine bacteria. Biochim Biophys Acta 1473:108–122
4. Merzendorfer H, Zimoch L (2003) Chitin metabolism in insects: structure, function and regulation of chitin synthases and chitinases. J Exp Biol 206:4393–4412
5. Herrera-Estrella A, Chet I (1999) Chitinases in biological control. EXS 87:171–184
6. Melchers LS, Stuiver MH (2000) Novel genes for disease-resistance breeding. Curr Opin Plant Biol 3:147–152
7. Gooday GW, Zhu WY, O'Donnell RW (1992) What are the roles of chitinases in the growing fungus? FEMS Microbiol Lett 100:387–392
8. Wills-Karp M, Karp CL (2004) Chitin checking—novel insights into asthma. N Engl J Med 351:1455–1457
9. Kawada M, Hachiya Y, Arihiro A et al (2007) Role of mammalian chitinases in inflammatory conditions. Keio J Med 56:21–27
10. Zhu Z, Zheng T, Homer RJ et al (2004) Elias acidic mammalian chitinase in asthmatic Th2 inflammation and IL-13 pathway activation. Science 304:1678–1682
11. Watanabe T, Suzuki K, OyaGi W et al (1990) Gene cloning of chitinase A1 from *Bacillus circulans* WL-12 revealed its evolutionary relationship to *Serratia* chitinase and to the type III homology units of fibronectin. J Biol Chem 265:15659–15665
12. Jones JDG, Grady KL, Suslow TV et al (1986) Isolation and characterization of genes encoding two chitinase enzymes from *Serratia marcescens*. EMBO J 5:6467–6473
13. Roffey PE, Pemberton JM (1990) Cloning and expression of an *Aeromonas hydrophila* chitinase gene in *Escherichia coli*. Curr Microbiol 21:329–337
14. Sitrit Y, Vorgias CE, Chet I et al (1995) Cloning and primary structure of The chiA gene from *Aeromonas caviae*. J Bacteriol 177:4187–4189
15. Tsujibo H, Orikoshi H, Tanno H et al (1993) Cloning, sequence, and expression of a chitinase gene from a marine bacterium, *Altermonas sp.* strain O-7. J Bacteriol 175:176–181
16. Suginta W (2007) Identification of chitin binding proteins and characterization of two chitinase isoforms from *Vibrio alginolyticus* 283. Enzyme Microb Tech 41:212–220
17. Itoi S, Kanomata Y, Koyama Y et al (2007) Identification of a novel endochitinase from a marine bacterium *Vibrio proteolyticus* strain No. 442. Biochim Biophys Acta 1774:1099–1107
18. Suzuki K, Sugawara N, Suzuki M et al (2002) Chitinases A, B, and C1 of *Serratia marcescens* 2170 produced by recombinant *Escherichia coli*: enzymatic properties and synergism on chitin degradation. Biosci Biotechnol Biochem 66:1075–1083
19. Sikorski P, Sørbotten A, Horn SJ et al (2006) *Serratia marcescens* chitinases with tunnel-shaped substrate-binding grooves show endo activity and different degrees of processivity during enzymatic hydrolysis of chitosan. Biochemistry 45:9566–9574
20. Suginta W, Vongsuwan A, Songsiriritthigul C et al (2004) An endochitinase A from *Vibrio carchariae*: cloning, expression, mass and sequence analyses, and chitin hydrolysis. Arch Biochem Biophys 424:171–180
21. Perrakis A, Tews I, Dauter Z et al (1994) Crystal structure of a bacterial chitinase at 2.3 Å resolution. Structure 2:1169–1180
22. Tews I, Terwisscha van Scheltinga AC, Perrakis A et al (1997) Substrate assisted catalysis unifies two families of chitinolytic enzymes. J Am Chem Soc 119:7954–7959
23. Terwisscha van Scheltinga AC, Armand S, Kalk KH et al (1995) Stereochemistry of chitin hydrolysis by a plant chitinase/lysozyme and X-ray structure of a complex with allosamidin: evidence for substrate assisted catalysis. Biochemistry 34:15619–15623
24. Hollis T, Monzingo AF, Bortone K et al (2000) The X-ray structure of a chitinase from the pathogenic fungus *Coccidioides immitis*. Protein Sci 9:544–551
25. Brameld KA, Goddard WA III (1998) Substrate distortion to a boat conformation at subsite -1 is critical in the mechanism of family 18 chitinases. J Am Chem Soc 120:3571–3580
26. Terwisscha van Scheltinga AC, Hennig M, Dijkstra BW (1996) The 1.8 Å resolution structure of hevamine, a plant chitinase/lysozyme, and analysis of the conserved sequence and structure motifs of glycosyl hydrolase family 18. J Mol Biol 262:243–257
27. Songsiriritthigul C, Pantoom S, Aguda AH et al (2008) Crystal structures of *Vibrio harveyi* chitinase A complexed with chitoo-ligosaccharides: implications for the catalytic mechanism. J Struct Biol 162:491–499
28. Uchiyama T, Katouno F, Nikaidou N et al (2001) Roles of the exposed aromatic residues in crystalline chitin hydrolysis by chitinase A from *Serratia marcescens* 2170. J Biol Chem 276:41343–41349
29. Sørbotten A, Horn SJ, Eijsink VG et al (2005) Degradation of chitosans with chitinase B from *Serratia marcescens*. Production of chitooligosaccharides and insight into enzyme processivity. FEBS J 272:538–549
30. Horn SJ, Sørbotten A, Synstad B et al (2006) Endo/exo mechanism and processivity of family 18 chitinases produced by *Serratia marcescens*. FEBS J 273:491–503
31. Boisset C, Fraschini C, Schülein M et al (2000) Imaging the enzymatic digestion of bacterial cellulose ribbons reveals the endo character of the cellobiohydrolase Cel6A from *Humicola insolens* and its mode of synergy with cellobiohydrolase Cel7A. Appl Environ Microbiol 66:1444–1452
32. Imai T, Boisset C, Samejima M et al (1998) Unidirectional processive action of cellobiohydrolase Cel7A on Valonia cellulose microcrystals. FEBS Lett 432:113–116
33. Imai T, Watanabe T, Yui T, Sugiyama J (2002) Directional degradation of beta-chitin by chitinase A1 revealed by a novel reducing end labelling technique. FEBS Lett 510:201–205
34. Suginta W, Vongsuwan A, Songsiriritthigul C et al (2005) Enzymatic properties of wild-type and active site mutants of chitinase A from *Vibrio carchariae*, as revealed by HPLC-MS. FEBS J 272:3376–3386

35. Suginta W, Songsiriritthigul C, Kobdaj A et al (2007) Mutations of Trp275 and Trp397 altered the binding selectivity of *Vibrio carchariae* chitinase A. Biochim Biophys Acta 1770:1151–1160

36. Laemmli UK (1970) Cleavage of structural proteins during the assembly of the head of bacteriophage T4. Nature 227:680–685

37. Bradford MM (1976) A rapid and sensitive method for the quantitation of microgram quantities of protein utilizing the principle of protein-dye binding. Anal Biochem 72:248–254

38. Miller GL (1959) Use of dinitrosalicylic acid reagent for determination of reducing sugar. Anal Chem 31:426–429

39. Armand S, Tomita H, Heyraud A et al (1994) Stereochemical course of the hydrolysis reaction catalysed by chitinase A1 and D from *Bacillus circulans* WL-12. FEBS Lett 343:177–180

40. Aronson NN Jr, Halloran BA, Alexyev MF et al (2003) Family 18 chitinase-oligosaccharide substrate interaction: subsite preference and anomer selectivity of *Serratia marcescens* chitinase A. Biochem J 376:87–95

41. Fukamizo T, Sasaki C, Schelp E et al (2001) Kinetic properties of chitinase-1 from the fungal pathogen *Coccidioides immitis*. Biochemistry 40:2448–2454

42. Sasaki C, Yokoyama A, Itoh Y et al (2002) Comparative study of the reaction mechanism of family 18 chitinases from plants and microbes. J Biochem 131:557–564

43. Pantoom S, Songsiriritthigul C, Suginta W (2008) The effects of the surface-exposed residues on the binding and hydrolytic activities of *Vibrio carchariae* chitinase A. BMC Biochem 9:2

44. Watanabe T, Ariga Y, Sato U et al (2003) Aromatic residues within the substrate-binding cleft of *Bacillus circulans* chitinase A1 are essential for hydrolysis of crystalline chitin. Biochem J 376:237–244